Experimental Investigation of a Double Layer Tensegrity Space Frame

Ioannis MITSOS
PhD Candidate
University of Cambridge
Department of Engineering
Advanced Structures Group
Cambridge, UK
im330@cam.ac.uk

Simon D. GUEST
Reader in Structural Mechanics
University of Cambridge
Department of Engineering
Advanced Structures Group
Cambridge, UK
sdg@eng.cam.ac.uk

Pete WINSLOW
Structural Engineer
Expedition Engineering
London, UK
Pete.w@expedition.uk.com

Bruce MARTIN
Structural Engineer
Associate Director
Expedition Engineering
London, UK
Bruce.m@expedition.uk.com

Summary

This paper describes an experimental investigation into a half-scale structural model of a solar collector double layer tensegrity space grid that was originally proposed to cover the new National Opera House in Athens, Greece. The structural scale model has a 5m span with cubic modules of 1.25m edge length. The key purpose of the experiment is to investigate the construction sequence, and, in particular, the pre-stressing of the structure. A novel pre-stressing scheme is used, where the top and bottom horizontal members are jacked apart, and a vertical compression member is lengthened. In practice, verification of pre-stressing is important, and a practical technique for measuring prestress in the diagonal members in the field through vibration measurements is described.

Keywords: *tensegrity; pre-stress; space grid; vibrations.*

1. Introduction

Stavros Niarchos Foundation Cultural Centre will be a new complex comprising the National Opera House in Athens, Greece. In this context, a Solar Collector Tensegrity Space Frame roof, inspired by Renzo Piano and designed by Expedition Engineering, was one of the proposed schemes (see Figure 1). The actual roof would be a 10,000 m^2 square structure covered with photovoltaic panels (see Figure 2). Considering the novelty of the design of this tensegrity roof, a 25 m^2 half-scale structural model had to be fabricated, built and investigated in the Structures Research Lab of the Department of Engineering at the University of Cambridge.

Although tensegrity structures are novel structures with high aesthetic impact, due to their poor structural performance they are limited to serve mainly artistic applications [1]. Moreover, there is a great debate around the definition of tensegrity structures with different researchers giving different definitions the past decades [see 2-5]. In this paper, the term 'tensegrity' refers to the inverse of the definition given by Motro, that is, "*tensegrity* are *systems in a stable selfstress state, they include a continuous set of compressed components inside a discontinuous set of tensioned components*"; it also fulfils the requirements set in Skelton's definition [4], which is ideal in order to comprehend the principles that tensegrity systems are based on.

The structural scale tensegrity model follows the latter definition being composed of a set of continuous cylindrical components and a set of discontinuous threaded rods, which were designed to act in compression and tension respectively. This paper investigates the structural model and

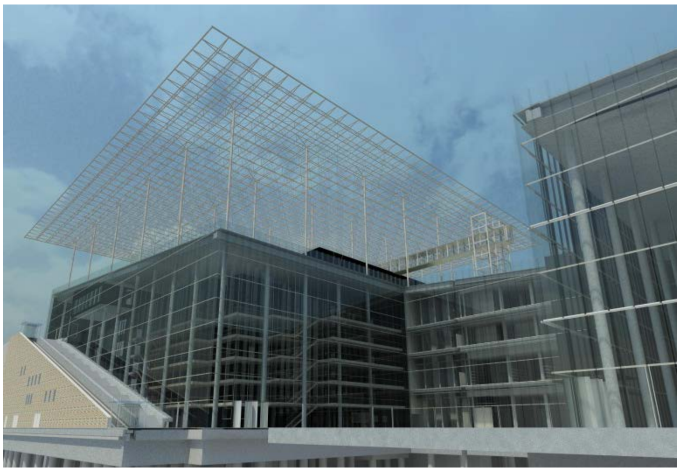

Fig. 1: Representation of the 10,000 m² tensegrity roof.

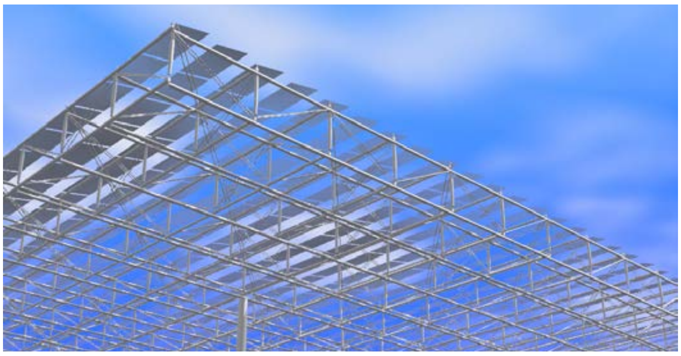

Fig. 2: Close view of the roof covered with PVP.

introduces a novel pre-stressing technique applied by lengthening the vertical compression components; a practical method for measuring the prestress in the tension members of a tensegrity space frame by measuring the natural frequency is described. The experimental results obtained from the pre-stress of the structural model were compared with a theoretical model based on linear elastic theory, whereas the experimental vibration measurements were compared with a theoretical formula [6] for transverse vibrations of beams subjected to axial forces.

2. Theoretical background

For the present study, matrix analysis of pre-stressed frameworks, as formulated by Pellegrino and Calladine (1986) and further used by many researchers [8,9], was used to determine the states of *selfstress* (*SS*) and the *internal mechanisms* (*IM*) of the tensegrity model.

For small perturbations and displacements of the pin-joints the governing relationships for the analysis of pre-stressed frameworks, such as tensegrity grids, can be linearized in the following equations:

$$[\mathbf{A}]\cdot\{\mathbf{t}\} = \{\mathbf{f}\} \quad (1)$$

where, [A] is the *equilibrium matrix*, t the tension vector and f the load vector. Since tensegrity structures are self-equilibrated structures, the external load vector f is zero, thus, eq.(1) takes the form:

$$[\mathbf{A}]\cdot\{\mathbf{t}\} = \{\mathbf{0}\} \quad (2)$$

Using eq.(2) or the nullspace of the equilibrium matrix A, one can determine the states of selfstress in the tensegrity system. From the *equilibrium matrix*, the *compatibility matrix* can be derived relating the elongations of the bars in an assembly with the components of displacements at the joints of each bar. Thus, the compatibility equations can be expressed as:

$$[\mathbf{C}]\cdot\{\mathbf{d}\} = \{\mathbf{e}\} \quad (3)$$

where C is the *compatibility* or *kinematic matrix* $(C = A^T)$, d the vector of node displacements and e the vector of variation coefficients (elongations). By simply taking the nullspace of C described by eq. (4) or the left-nullspace of A, the independent inextensional mechanisms of the assembly can be determined.

$$[\mathbf{C}]\cdot\{\mathbf{d}\} = \{\mathbf{0}\} \quad (4)$$

Using the equilibrium and compatibility matrices through equations 2 & 4 for the analysis of the double layer tensegrity grid, it was observed that the specific geometric configuration yields a 2×2 *minimal grid*. The latter simply implies that the 2×2 grid shown in Figure 3 is the first linear combination of this type of module geometric configuration, which has a single state of selfstress [10]. In addition to that, it was found that the *minimal grid* possesses four internal mechanisms giving an insight in to the structural behaviour. Following the same method the *SS* and *IM* of the actual 4×4 half-scale structural model shown in Figure 4 were found to possess $SS = 9$ and $IM = 8$.

3. Experimental procedure

The experimental procedure was divided in two phases. The first phase (I) was the assembly, monitoring setup, pre-stressing and loading. The second phase (II) included the measurement of the tensile load in the diagonals using structural acoustics.

3.1 Experimental phase I

The first stage of the experimental procedure was the assembly of the structural model using the fabricated structural elements. For the assembly process, two main types of structural elements were used:

i. Steel circular hollow sections 60×3×1250 mm (outside diameter, thickness, length) with conical pieces and 16mm studding extensions fitted at the end.
ii. 8.8 grade steel threaded rods with 12mm diameter (10mm solid core).

Before the assembly of the model, each member of the structure, both vertical and diagonal, had strain gauges and labels attached in order to monitor the behaviour of each element independently during the testing. The assembly of the model was carried out in six stages, as illustrated in Figure 5, and it was followed by the setup of the monitoring, where the strain gauges were wired and connected in to the data loggers and a PC.

3.1.1 Pre-stressing

A novel technique for the pre-stressing of the 4×4 structural model was employed by adjusting the length of the vertical components. The concept was that the vertical compression components would be jacked apart and a spacer with specified thickness would extend the length of the members inducing the pre-stress in the diagonal tension rods. The jacking process could be achieved following two different methods. The first method to achieve the length extension of the vertical components is by setting up a jack, as shown in Figure 6 (a), and expanding the jack to create a gap where the spacer

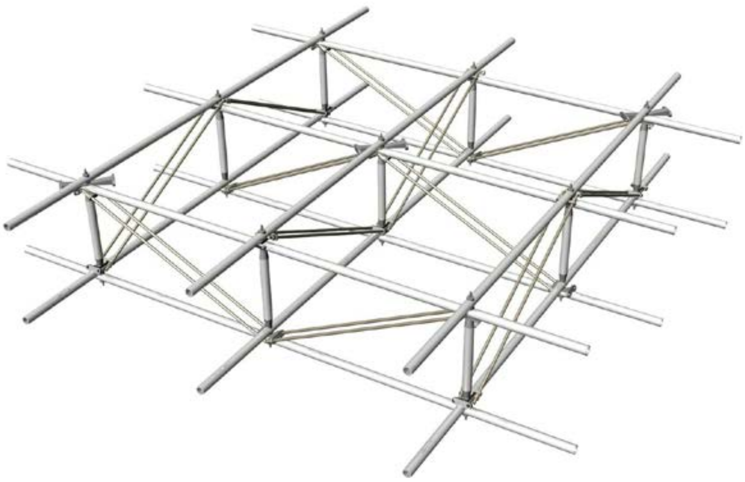

Fig. 3: The 2×2 double layer tensegrity grid with SS=1 and IM=4.

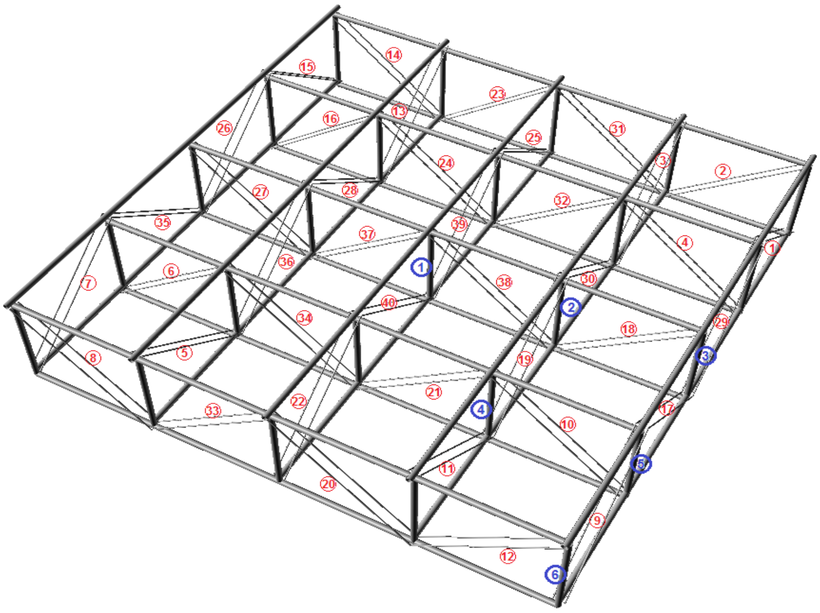

Fig. 4: The 4×4 structural scale model possessing SS=9 and IM=8.

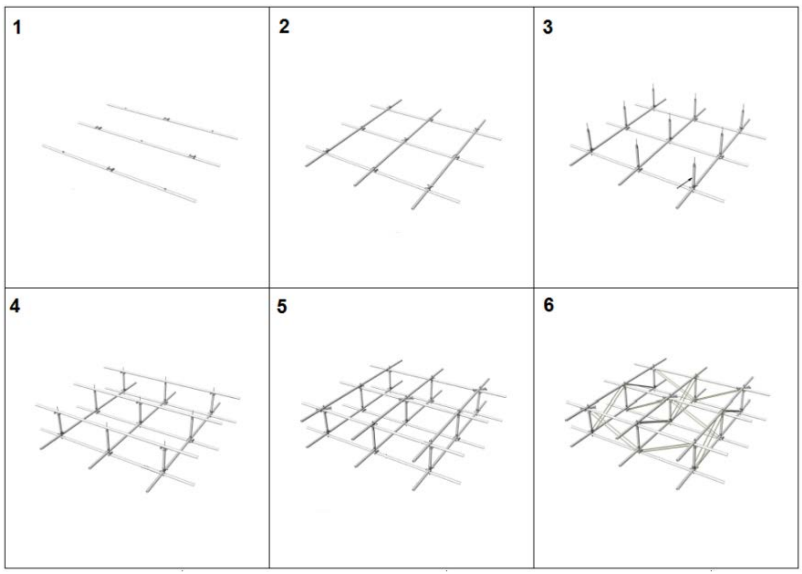

Fig. 5: Assembly stages.

of specified thickness would be inserted (see Figure 6-b). The second jacking technique required a jack between the top and bottom horizontal tubes, pushing them apart in order create the gap. The extension, in this case, is induced with the turning of a bolt placed at the position of the gap during the assembly of the grid.

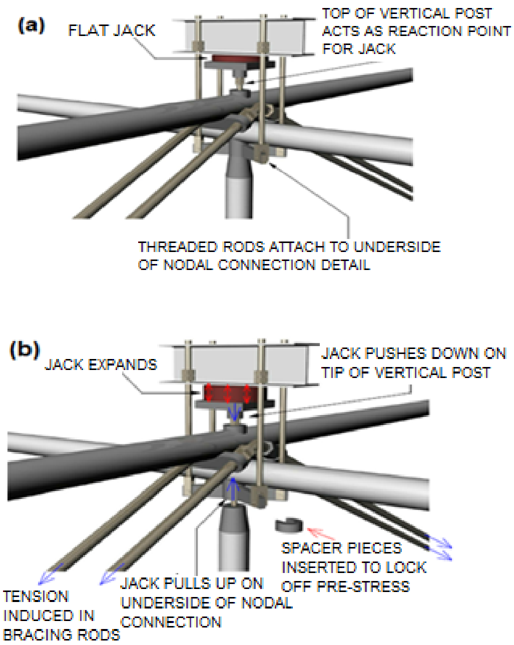

Fig. 6: Jacking method 1. (a)The jack is set up on node of the vertical post, (b) the jack pushes the tip of the extending rod and a spacer creates the extension.

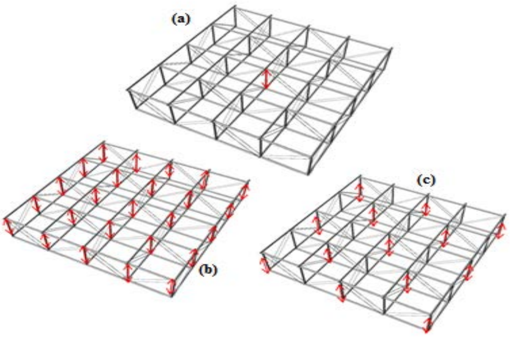

Fig. 7: Pre-stressing patterns.

Thus, with the use of the aforementioned pre-stressing technique, the model was tested in order to investigate the effect of three different pre-stressing patterns on the grid. To achieve the latter, the following pre-stressing patterns were examined by extending (see Figure 7):

a. the central vertical member;
b. all the vertical members;
c. the verticals in a checkerboard pattern.

A theoretical model for the analysis of statically indeterminate truss structures has been given by Livesley, 1974, and it is based on *Force method*. The latter method is appropriate for deflections lying within the elastic region as the ones observed in the present study. Thus, the experimental results obtained in this study are compared with a theoretical model in order to get a better insight about the structural behaviour of the structure.

The results of a 2mm length extension, using the pre-stressing pattern (b) shown in Figure 7, are presented in Figure 8. The latter shows the loads on the pairs of the diagonal tension members induced by the extension of all the vertical compression components. The element reference number axis represents the diagonal pairs which are referenced with the labels assigned in Figure 4 (red labels). However, due to the symmetry of the grid only the elements of a quarter of the structure are presented in Figures 8-9. Figure 9 represents the compressive load imparted in the vertical members from their own length extension. The six elements presented in Figure 9 are referenced with blue labels in Figure 4 and they were chosen as indicative due to the symmetry of the structure.

From the results depicted in Figures 8-9 it can be deduced that the experimental tensegrity model presents the similar trend with the theoretical model with slight deviations. From the analysis carried out it was observed that the average deviation between the two models was approximately 5% - 15%. The deviations observed between the experimental and the theoretical loads were attributed mostly to errors occurring from the variation in the geometry and stiffness of the fabricated elements. Among the three pre-stressing

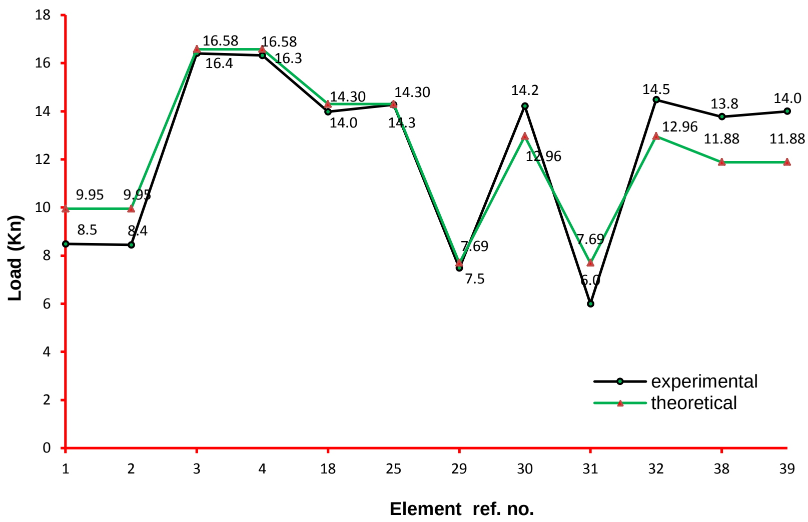

Fig. 8: Theoretical vs Experimental tensile loads carried by the diagonal pairs after a 2mm extension using pre-stressing technique (b).

patterns mentioned above (a-c), pattern b seem to be the optimal pre-stressing pattern for the frame with the present geometric configuration. Techniques (a) and (c) do not induce adequate and uniform prestress along the beam comparing to (a) which induce a uniform pre-stress along the grid leading to a stiff and stable system.

To further investigate the structural behaviour of the structural model, a loading test was carried out while the model was pre-stressed with a 2mm extension using pattern (b). The grid was loaded with a 12.7 kN downward load applied on the central node of the bottom layer. The diagonal element forces induced by the combination of the pre-stress and the nodal force applied are shown in Figure 10. In the latter figure representative elements of half the structure (the 2×4 grid) are presented due to symmetry. The average deviation between theoretical and experimental element loads increased to 15% with the presence of the applied load on the grid. The latter increase shows that the average deviation produced from the variation in the geometry and stiffness of the fabricated elements is proportional to the load. Despite the deviation recorded in the results one could say that the behaviour of the structural model was successfully predicted from the theoretical model.

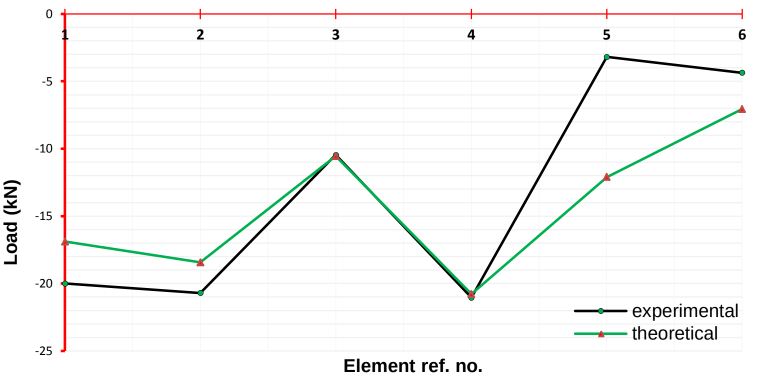

Fig. 9: Theoretical vs Experimental compressive loads carried by the vertical elements after a 2mm extension using pre-stressing technique (b).

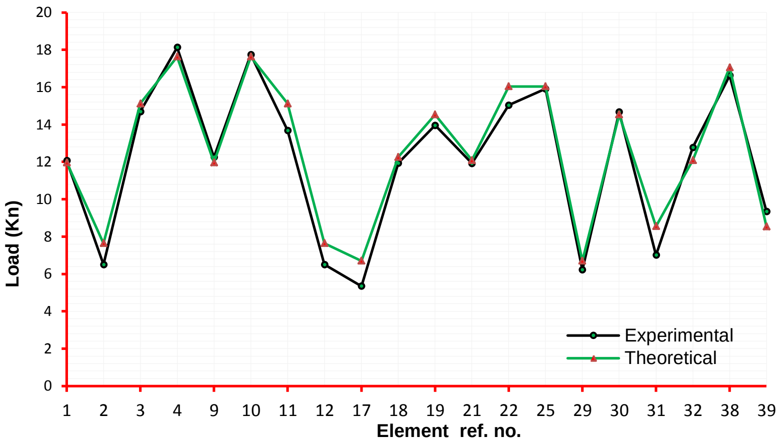

Fig. 10: Theoretical vs Experimental compressive loads carried by the vertical elements after a 2mm extension and a 12.7 kN applied load using pre-stressing technique (b).

3.2 Experimental phase II

The prestress of the diagonal tension members of the tensegrity space frame is the key factor for its structural behaviour. Thus, a robust method for measuring the tensile load on the diagonal members was employed using elements of vibration analysis.

A theoretical model for the transverse vibration of axially stressed beams has been provided by Timoshenko et al., 1974, which is appropriate for the frequency range of the measurements presented here and with which one can compare results. Considering that the tensile rod is simply supported, the corresponding angular frequency for every natural mode of vibration can be obtained by eq.(5)

$$\omega_n = \frac{n^2\pi^2\alpha}{l^2}\sqrt{1+\frac{Sl^2}{n^2EI\pi^2}}, \quad (n = 1,2,3 \ldots \infty) \qquad (5)$$

where, n is the natural mode of vibration, l the longitudinal length of the element, S the axial tensile load and $\alpha = \sqrt{EI/\rho A}$. From eq. (5) it is apparent that by increasing S the natural frequency increases as the tensile force stiffens the beam. Rearranging eq. (5), the tensile load can be determined when

ω_n and *n* are the arithmetic variables as shown in eq. (6). The latter can be employed to predict the tension in a pre-stressed member when the natural frequency of the corresponding vibration mode is experimentally measured.

$$S = \frac{EI}{(ln\pi)^2}\left(\frac{l^4\omega_n^2}{\alpha^2} - n^4\pi^4\right), \quad (n = 1,2,3 \dots \infty) \qquad (6)$$

3.2.1 Vibration experiment

The experimental readings recorded correspond to a 1.6 ± 0.005 m long and 5 ± 0.1 mm diameter thick steel rod identical to the ones used in the experimental space frame. The experiment was carried out by setting up a rig where the steel rod was stretched to a certain load. The latter was pre-stressed using tightening bolts at the ends which were setup to act as pinned joints and the pre-stressing was recorded by a low profile 50 kN capacity load transducer with ±0.01% accuracy. An impact hammer with a soft rubber face was used to produce an acoustic wave which was collected by a sensitive (65dB±2) microphone (Figure 11). The microphone was placed in the mid-span of the rod at ~15mm vertical distance underneath the rod where the impact was applied and it was directly connected to a 24-bit/96kHz audio resolution soundcard of a PC station which was recording and analysing the input data. The recording time was 3 sec with sampling rate 96 kHz, the standard sampling rate of the soundcard. Measurements were made in a laboratory with room temperature (~20 ^{o}C) and reduced noise.

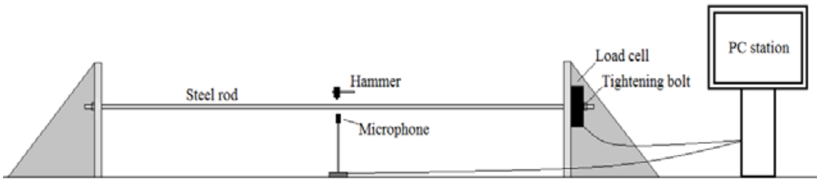

Fig.11: Diagram of the experimental setup used to obtain the acoustic resonance spectrum of the cylindrical tension rod when stretched to a certain tensile load.

Since the main goal of this experiment was to examine the reliability of the transverse vibrations method for measuring loads of axially pre-stressed rods, a number of vibration measurements were taken to determine the natural frequency of the rod for a tensile load range 0-20 kN. To determine the natural frequency of the pre-stressed rod subject to various axial tensile loads, the resonance spectrum had to be obtained. Thus, a Fast Fourier Transform (FFT) analysis together with the use of the time-varying spectrum, or sonogram, which has been used with success for studies in structural acoustics [12], was employed to determine the natural frequency of the pre-stressed rod. Figure 12(a) shows a typical FFT spectrum, in the range of 0-650 Hz, collected in the experiment while the rod was axially loaded with a 20 kN tensile load. In that range, the distinguished picks representing the vibration frequency modes can be observed. Figure 12(b) is a FFT spectrum showing the first natural mode of vibration of the 20 kN pre-stressed rod.

3.2.2 Vibration measurements

For the same amount of load the sonogram was calculated by simply taking portions of the time series, and undertaking a Fourier analysis. Then, the results were plot as a two-dimensional picture of a power-spectral surface picture. The sonogram calculated for the 20 kN pre-stressing case was plotted in a contour surface plot which includes amplitude levels. The sonogram is considered to be a very advantageous approach since it yields information without using any *priori* knowledge about the system being studied [12]. Figure 13, clearly shows the first natural vibration mode to be excited at 55.77 Hz. The latter measurement was validated using the theoretical formula in eq.(5). Setting *n*=1 and *S*=20 Kn, eq.(5) yields the theoretical natural frequency for the first natural vibration mode to be equal to 57.14 Hz. The latter presents a deviation lower than 5% which rests within the limits of acceptable error. A complementary plot to verify the value of ω_n is shown in Figure 14. The latter depicts the fitted values of the first vibration mode shown in Figure 13. This graph is produced by taking the cross section at a pick with a particular frequency in the sonogram and fitting a single decaying sine wave to give the frequency. This fitted values plot is to verify the existence of the vibration mode at the particular natural frequency using as indicator the *rsqph* which is the reliability factor for the frequency fit. In the particular loading case (20 kN), the *rsqph* factor was 0.999867 indicating that the result from the sonogram for the first vibration mode is correct.

As previously stated, the measurements were made on a steel rod, subjected to loads lying in the range of 0-20 kN (4 kN increments). The data tabulated in Table 1, show the theoretical values of ω_n obtained by using eq.(5) for the corresponding values of S and n=1, and the experimental values of ω_n corresponding to the first natural vibration mode. Figure 15 depicts the relationship between the theoretical and the experimental values of ω_n for a specific set of axial tension loads applied on the steel rod. From that graph it could be observed that almost all the experimental frequency values lie within the range of 5% deviation compared with the theoretical model presented by eq.(5).

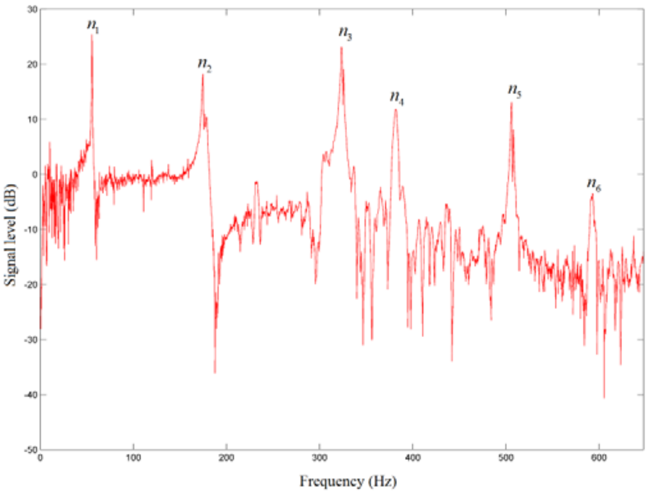

Fig.12(a): Resonance spectrum (0-650 Hz) of a 20 kN pre-stressed rod

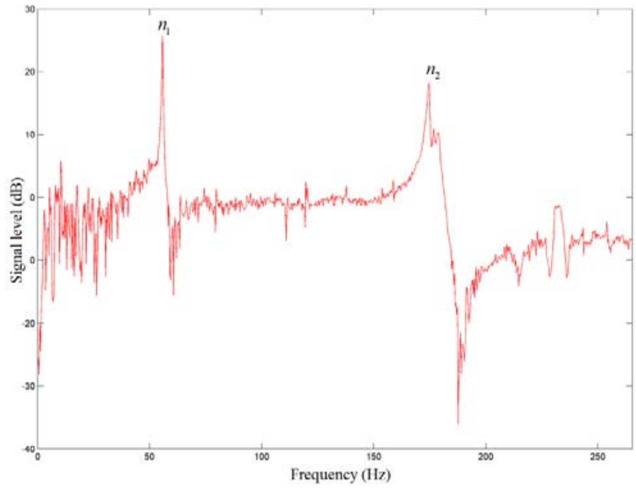

Fig.12 (b): Resonance spectrum (0-250 Hz) of a 20 kN pre-stressed rod.

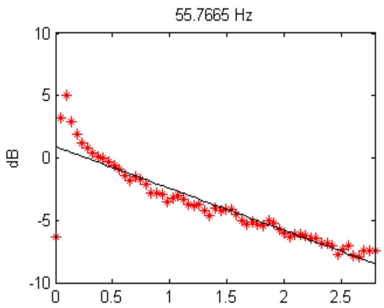

Fig.14: Fitted values for n_1.

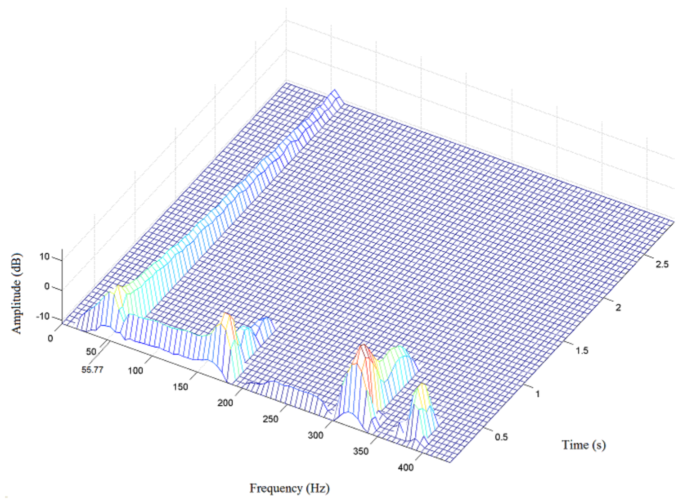

Fig.13: Sonogram surface plot showing the natural modes of vibration in a range 0-400 Hz.

From the results obtained from the vibration experiment, it can be deduced that one can predict with a reliable accuracy the natural frequency of pre-stressed rods and furthermore determine the tensile load applied on the rods just by plugging the value of ω_n in eq.(6). Thus, using the principles of this experiment, a reliable method for measuring the tension of pre-stressed elements can be used in *situ* when a tensegrity space frame is under construction.

4 Conclusions

This study showed a novel pre-stressing technique and a practical method to measure the load of members subjected to tensile loads. The pre-stressing technique presented in this paper was successfully applied to the experimental tensegrity double layer grid and the behaviour of the experimental model was predicted relatively accurately by a theoretical model based on linear elastic theory. The method for measuring the load on tension components *in situ* using structural acoustics was reliable to 5% accuracy according to a theoretical model based on linear vibration theory.

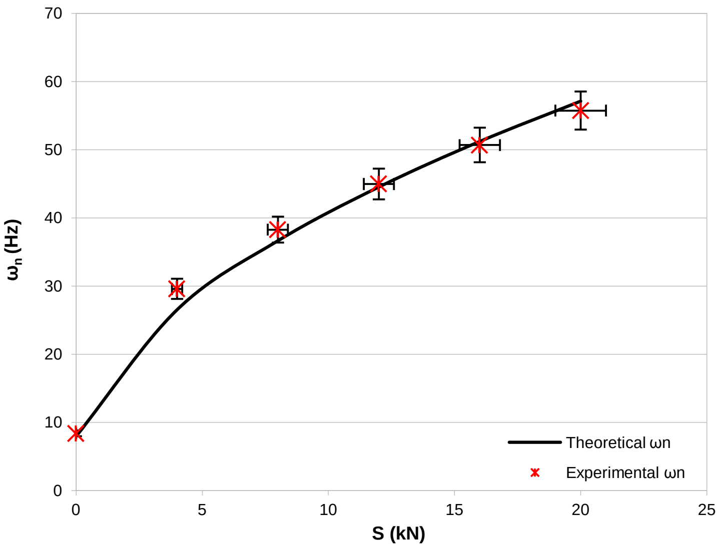

Fig.15: Experimental ω_n with 5% error bars fitted on the theoretical curve produced from eq. (1).

Table 1:Natural frequencies for 0-20 kN axial loads

S (kN)	Theoretical ω_n (Hz)	Experimental ω_n (Hz)
0	7.98	8.40
4	26.53	29.60
8	36.66	38.30
12	44.55	45.00
16	51.23	50.70
20	57.14	55.76

5 Acknowledgements

This work has been carried out with the support of *Stavros Niarchos Foundation Cultural Center (SNFCC)*. The authors are particularly grateful, to Jim Woodhouse Professor of Vibrations at Cambridge University for his support and insightful comments concerning the vibration experiment, and Jessica Dower for her assistance during the experimental procedure. The first author is funded for his research studies by *Alexander S. Onassis Public Benefit Foundation*.

6 References

[1] SNELSON, K. (2009). *Kenneth Snelson: Forces Made Visible.* Lenox, Massachusetts: Hudson Hills Press LLC.

[2] PUGH, A. (1976). *An introduction to tensegrity.* Berkeley, CA: University of California Press.

[3] MOTRO, R. (2003). *Tensegrity: Structural systems of the future.* London, UK: Kogan Page Science.

[4] SKELTON, R. E., & DE OLIVEIRA, M. C. (2009). *Tensegrity systems.* New York: Springer Science.

[5] WANG, B. B. (2004). *Free standing tension structures.* Oxford: Spon Press.

[6] TIMOSHENKO, S., YOUNG, D. H., & WEAVER, J. (1974). *Vibration problems in engineering* (4 ed.). Palo Alto, California, USA: John Wiley & Sons, Inc.

[7] PELLEGRINO, S., & CALLADINE, C. R. (1986). Matrix analysis of statically and kinematically indeterminate frameworks. *International Journal of Solids and Structures, 22*(2), 409-428.

[8] KANGWAI, R. D., & GUEST, S. D. (1999). Detection of finite mechanisms in symmetric structures. *International Journal of Solids and Structures, 36*(36), 5507 - 5527.

[9] QUIRANT, J., KAZI-AOUAL, M. N., & MOTRO, R. (2003). Designing tensegrity systems: the case of a double layer grid. *Engineering Structures, 25*(9), 1121 - 1130.

[10] MITSOS, I. (2010). *Structural behaviour of double-layer tensegrity grids.* University of Cambridge, CUED. Cambridge, UK: Research report.

[11] LIVESLEY, R. K. (1975). *Matrix methods of structural analysis.* Oxford, UK: Pergamon Press Ltd.

[12] HODGES, C. H., POWER, J., & WOODHOUSE, J. (1984). The use of sonogram in structural acoustics and an application the vibrations of cylindrical shells. *Journal of Sound and Vibration, 101*(2), 203-218